

Origin of the High Piezoelectric Response in $\text{PbZr}_{1-x}\text{Ti}_x\text{O}_3$

R. Guo,¹ L. E. Cross,¹ S-E. Park,¹ B. Noheda,^{2,3,*} D. E. Cox,³ and G. Shirane³

¹Materials Research Laboratory, Pennsylvania State University, University Park, Pennsylvania 16802-4800

²Departamento de Física de Materiales, Universidad Autónoma de Madrid, 28049 Madrid, Spain

³Physics Department, Brookhaven National Laboratory, Upton, New York 11973-5000

(Received 14 December 1999)

High resolution x-ray powder diffraction measurements on poled $\text{PbZr}_{1-x}\text{Ti}_x\text{O}_3$ (PZT) ceramic samples close to the rhombohedral-tetragonal phase boundary (the so-called morphotropic phase boundary) have shown that for both rhombohedral and tetragonal compositions the piezoelectric elongation of the unit cell does not occur along the polar directions but along those directions associated with the monoclinic distortion. This work provides the first direct evidence for the origin of the very high piezoelectricity in PZT.

PACS numbers: 77.84.Dy, 61.10.-i, 77.65.-j

The ferroelectric $\text{PbZr}_{1-x}\text{Ti}_x\text{O}_3$ (PZT) system has been extensively studied because of its interesting physical properties close to the morphotropic phase boundary (MPB), the nearly vertical phase boundary between the tetragonal and rhombohedral regions of the phase diagram close to $x = 0.50$, where the material exhibits outstanding electromechanical properties [1]. The existence of directional behavior for the dielectric and piezoelectric response functions in the PZT system has been predicted by Du *et al.* [2,3] from a phenomenological approach [4]. These authors showed that for rhombohedral compositions the piezoelectric response should be larger for crystals oriented along the [001] direction than for those oriented along the [111] direction. Experimental confirmation of this prediction was obtained [5–7] for the related ferroelectric relaxor system $\text{PbZn}_{1/3}\text{Nb}_{2/3}\text{-PbTiO}_3$ (PZN-PT), which has a rhombohedral-to-tetragonal MPB similar to that of PZT, but it has not been possible to verify similar behavior in PZT due to the lack of single crystals. Furthermore, *ab initio* calculations based on the assumption of tetragonal symmetry, that have been successful for calculating the piezoelectric properties of pure PbTiO_3 [8–11], were unable to account for the much larger piezoelectric response in PZT compositions close to the MPB. Thus, it is clear that the current theoretical models lack some ingredient which is crucial to understanding the striking piezoelectric behavior of PZT.

The stable monoclinic phase recently discovered in the ferroelectric $\text{PbZr}_{1-x}\text{Ti}_x\text{O}_3$ system (PZT) close to the MPB [12] provides a new perspective to view the rhombohedral-to-tetragonal phase transformation in PZT and in other systems with similar phase boundaries as PMN-PT and PZN-PT [13]. This phase plays a key role in explaining the high piezoelectric response in PZT and, very likely, in other systems with similar MPBs. The polar axis of this monoclinic phase is contained in the (110) plane along a direction between that of the tetragonal and rhombohedral polar axes [12]. An investigation of several compositions around the MPB has suggested a

modification of the PZT phase diagram [1] as shown in Fig. 1 (top right) [13].

A local order different from the long-range order in the rhombohedral and tetragonal phases has been proposed from a detailed structural data analysis. Based on this, a model has been constructed in which the monoclinic

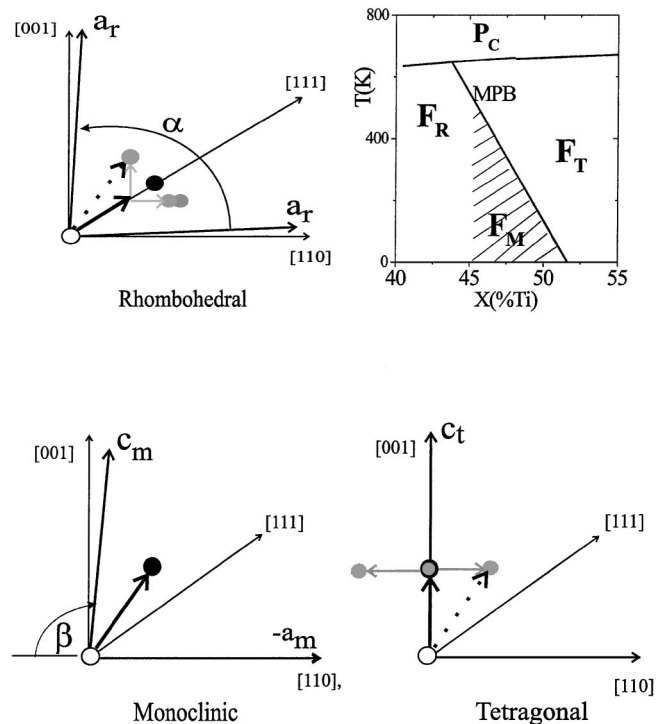


FIG. 1. Schematic view of the PZT phase diagram in the vicinity of the MPB showing the monoclinic region (top right). A projection of the rhombohedral (top left), monoclinic (bottom left), and tetragonal (bottom right) unit cells on the pseudocubic (110) plane is sketched. The solid circles represent the observed lead shifts with respect to the ideal cubic structure and the grey circles the locally disordered shifts, four in the tetragonal phase and three in the rhombohedral phase. The heavy dashed arrows represent the freezing-out of one of these shifts to give the observed long-range monoclinic structure [13].

distortion (Fig. 1, bottom left) can be viewed as either a condensation along one of the $\langle 110 \rangle$ directions of the local displacements present in the tetragonal phase [13] (Fig. 1, bottom right), or as a condensation of the local displacements along one of the $\langle 100 \rangle$ directions present in the rhombohedral phase [14] (Fig. 1, top left). The monoclinic structure, therefore, represents a bridge between these two phases and provides a microscopic picture of the MPB region [13].

In the present work experimental evidence of an enhanced elongation along [001] for rhombohedral PZT and along [101] for tetragonal PZT ceramic disks revealed by high resolution x-ray diffraction measurements during and after the application of an electric field is presented. This experiment was originally designed to address the question whether poling in the MPB region would simply change the domain population in the ferroelectric material, or whether it would induce a permanent change in the unit cell. As shown below, from measurements of selected peaks in the diffraction patterns, a series of changes in the peak profiles from the differently oriented grains are revealed which provide key information about the PZT problem.

$\text{PbZr}_{1-x}\text{Ti}_x\text{O}_3$ ceramic samples with $x = 0.42$, 0.45 , and 0.48 were prepared by conventional solid-state reaction techniques using high purity (better than 99.9%) lead carbonate, zirconium oxide, and titanium oxide as starting compounds. Powders were calcined at 900°C for 6 h and recalcined as appropriate. After milling, sieving, and the addition of the binder, the pellets were formed by uniaxial cold pressing. After burnout of the binder, the pellets were sintered at 1250°C in a covered crucible for 2 h, and furnace cooled. During sintering, PbZrO_3 was used as a lead source in the crucible to minimize volatilization of lead. The sintered ceramic samples of about 1 cm diameter were ground to give parallel plates of 1 mm thickness, and polished with $1\ \mu\text{m}$ diamond paste to a smooth surface finish. To eliminate strains caused by grinding and polishing, samples were annealed in air at 550°C for 5 h and then slow cooled. Silver electrodes were applied to both surfaces of the annealed ceramic samples and air dried. Disks of all compositions were poled under a dc field of $20\ \text{kV/cm}$ at 125°C for 10 min and then field cooled to near room temperature. The electrodes were then removed chemically from the $x = 0.42$ and 0.48 samples. For the $x = 0.45$ sample (which had been ground to a smaller thickness, about 0.3 mm), the electrodes were retained, so that diffraction measurements could be carried out under an electric field.

Several sets of high-resolution synchrotron x-ray powder diffraction measurements were made at beam line X7A at the Brookhaven National Synchrotron Light Source. A $\text{Ge}(111)$ double-crystal monochromator was used in combination with a $\text{Ge}(220)$ analyzer, with a wavelength of about $0.8\ \text{\AA}$ in each case. In this configuration, the instrumental resolution, $\Delta 2\theta$, is an order-of-magnitude better than that of a conventional laboratory instrument (better than 0.01° in the 2θ region 0° – 30°). The poled and un-

poled pellets were mounted in symmetric reflection geometry and scans made over selected peaks in the low-angle region of the pattern. It should be noted that since lead is strongly absorbing, the penetration depth below the surface of the pellet at $2\theta = 20^\circ$ is only about $2\ \mu\text{m}$. In the case of the $x = 0.45$ sample, the diffraction measurements were carried out with an electric field applied *in situ* via the silver electrodes.

Powder diffraction measurements on a flat plate in symmetric reflection, in which both the incident and the diffracted wave vectors are at the same angle, θ , with the sample plate, ensures that the scattering vectors are perpendicular to the sample surface. Thus only crystallites with their scattering vector parallel to the applied electric field are sampled. Scans over selected regions of the diffractogram, containing the (111), (200), and (220) pseudocubic reflections, are plotted in Fig. 2 for poled and unpoled PZT samples with the compositions $x = 0.48$ (top) and $x = 0.42$ (bottom), which are in the tetragonal and rhombohedral regions of the phase diagram, respectively. The diffraction profiles of the poled and unpoled samples show very distinctive features. For the tetragonal composition (top), the (200) pseudocubic reflection (center) shows a large increase in the tetragonal (002)/(200) intensity ratio after poling due to the change in the domain population,

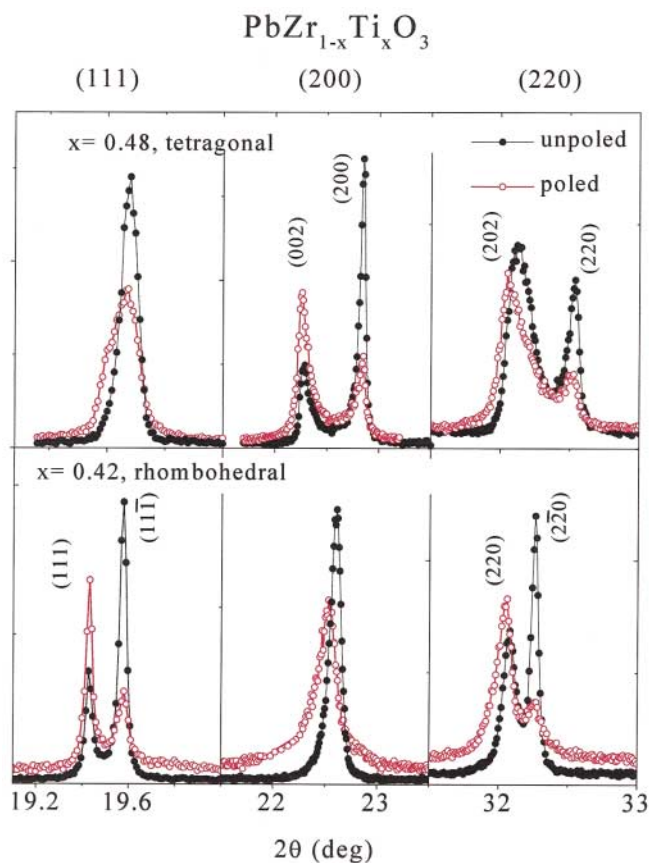


FIG. 2 (color). Comparison of (111), (200), and (220) pseudocubic reflections for the $x = 0.48$ (tetragonal), and $x = 0.42$ (rhombohedral) PZT compositions before and after poling.

which is also reflected in the increased (202)/(220) intensity ratio in the right side of the figure. In the rhombohedral composition with $x = 0.42$ (bottom of Fig. 2), the expected change in the domain population can be observed from the change of the intensity ratios of the rhombohedral (111) and ($\bar{1}\bar{1}\bar{1}$) reflections (left side) and the (220) and ($\bar{2}\bar{2}\bar{0}$) reflections (right side).

In addition to the intensity changes, the diffraction patterns of the poled samples show explicit changes in the peak positions with respect to the unpoled samples, corresponding to specific alterations in the unit cell dimensions. In the rhombohedral case ($x = 0.42$), the electric field produces no shift in the (111) peak position (see bottom left plot in Fig. 2), indicating the absence of any elongation along the polar directions after the application of the field. In contrast, the poling does produce a notable shift of the (00l) reflections (center plot), which corresponds to a very significant change of d spacing, with $\Delta d/d = 0.32\%$, $\Delta d/d$ being defined as $(d_p - d_u)/d_u$, where d_p and d_u are the d spacings of the poled and unpoled samples, respectively. This provides experimental confirmation of the behavior predicted by Du *et al.* [3] for rhombohedral PZT, as mentioned above. The induced change in the dimensions of the unit cell is also reflected as a smaller shift in the (202) reflection (right side plot), corresponding to a $\Delta d/d$ along [101] of 0.12%.

In the tetragonal case for $x = 0.48$ (top of Fig. 2), there is no peak shift observed along the polar [00l] direction (center plot), but the (202) and the (111) reflections exhibit striking shifts (right and left sides, respectively). Furthermore, this composition, which at room temperature is just at the monoclinic-tetragonal phase boundary, shows, after poling, a clear tendency towards monoclinic symmetry, in that the (111) and (202) reflections, already noticeably broadened in the unpoled sample and indicative of an incipient monoclinicity, are split after poling. These data clearly demonstrate, therefore, that whereas the changes induced in the unit cell after the application of an electric field do not increase either the rhombohedral or the tetragonal strains, a definite elongation is induced along those directions associated with the monoclinic distortion.

In addition to the measurements on the poled and unpoled samples, diffraction measurements were performed *in situ* on the rhombohedral PZT sample with $x = 0.45$ as a function of applied electric field at room temperature. The results are shown in Fig. 3 where the (111), (200), and (220) pseudocubic reflections are plotted with no field applied (top) and with an applied field of 59 kV/cm field (bottom). The top part of the figure also shows data taken after removal of the field. As can be seen, measurements with the field applied show no shift along the polar [111] direction but, in contrast, there is a substantial shift along the [001] direction similar to that for the poled sample with $x = 0.42$ shown in Fig. 2, proving that the unit cell elongation induced by the application of a field during the poling process corresponds to the piezoelectric effect induced by the *in situ* application of a field. Comparison of the two

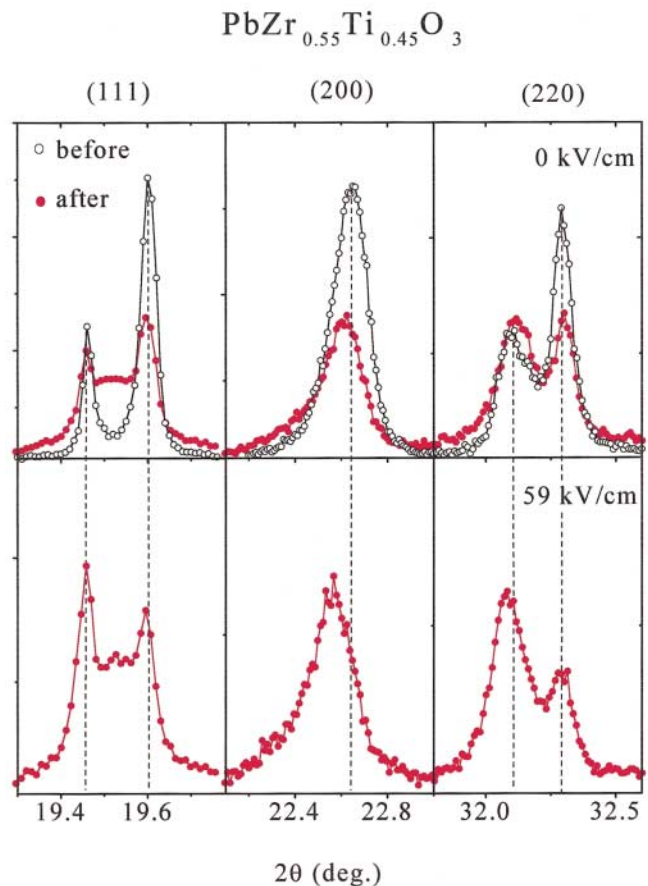


FIG. 3 (color). (111), (200), and (220) pseudocubic reflections for PZT with $x = 0.45$ measured on an unpoled sample (open circles) and on a similar sample after the application and removal of a field of 59 kV/cm at room temperature (solid circles) are plotted in the upper part of the figure. The scattered intensity at $2\theta = 19.52^\circ$ from the second sample corresponds to the (111) reflection from the silver electrode. Measurements on the latter sample under an electric field of 59 kV/cm applied *in situ* are plotted in the lower part of the figure.

sets of data for $x = 0.45$ before and after the application of the field shows that the poling effect of the electric field at room temperature is partially retained after the field is removed, although the poling is not as pronounced as for the $x = 0.42$ sample in Fig. 2.

A quantification of the induced microstrain along the different directions has been made by measuring the peak shifts under fields of 31 and 59 kV/cm. In Fig. 4, $\Delta d/d$ is plotted *versus* the applied field, E , for the (200) and (111) reflections. These data show an approximately linear increase in $\Delta d/d$ for (200) with field, with $\Delta d/d = 0.30\%$ at 59 kV/cm, corresponding to a piezoelectric coefficient $d_{33} \approx 500$ pm/V, but essentially no change in the d spacing for (111).

It is interesting to compare in Fig. 4 the results of dilatometric measurements of the macroscopic linear elongation ($\Delta l/l$) on the same pellet, which must also reflect the effects of domain reorientation. At higher fields, this contribution diminishes and one could expect the $\Delta l/l$ vs E curve to fall off between those for the [100] and [111]

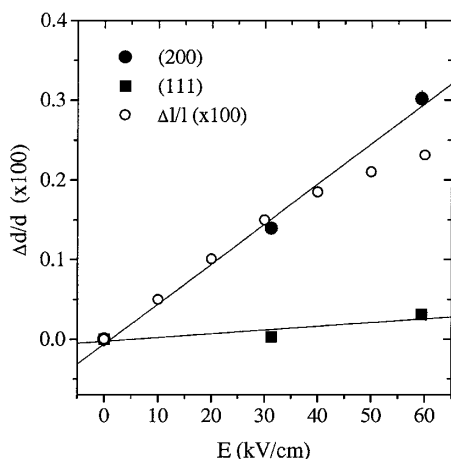


FIG. 4. Fractional change of d spacing, $\Delta d/d$ for PZT with $x = 0.45$ from the rhombohedral (200) and (111) reflections as a function of electric field (closed symbols). Dilatometric measurements of the macroscopic $\Delta l/l$ for the same pellet are also shown (open circles).

oriented grains, typical of the strain behavior of polycrystalline ceramics [15]. Although such a trend is seen above 30 kV/cm, it is intriguing to note that below this value, the macroscopic behavior is essentially the same as the microscopic behavior for the (200) reflection.

It is of interest to relate our observations to the more conventional description of piezoelectric effects in ceramics, in which the dielectric displacements would be attributed to tilts of the polar axis. What we actually observe in the diffraction experiment is an intrinsic monoclinic deformation of the unit cell as a consequence of the rotation of the polar axis in the monoclinic plane. However, large atomic displacements can occur only in compositions close to the MPB, and it is this feature which accounts for the sharp peak in the piezoelectric d constants for compositions close to 52:48 Zr/Ti [1].

We therefore conclude that the piezoelectric strain in PZT close to the morphotropic phase boundary, which produces such striking electromechanical properties, is not along the polar directions but along those directions associated with the monoclinic distortion. This work supports a model based on the existence of local monoclinic shifts superimposed on the rhombohedral and tetragonal displacements in PZT which has been proposed from a detailed structural analysis of tetragonal [13] and rhombohedral [14] PZT samples. Very recent first-principle calculations by Bellaiche *et al.* [16] have been able not only to reproduce the monoclinic phase but also to explain the high piezoelectric coefficients by taking into account rotations in the monoclinic plane.

As demonstrated above, these high resolution powder data provide key information to understanding the piezoelectric effect in PZT. In particular, they allow an accurate determination of the elongation of the unit cell along the direction of the electric field, although they give no information about the dimensional changes occurring along the perpendicular directions, which would give a more com-

plete characterization of the new structure induced by the electric field. It is interesting to note that in the case of the related ferroelectric system PZN-PT, the availability of single crystals has allowed Durbin *et al.* [7] to carry out diffraction experiments along similar lines at a laboratory x-ray source. Synchrotron x-ray experiments by the present authors are currently being undertaken on PZN-PT single crystals with Ti contents of 4.5 and 8% under an electric field, and also on other ceramic PZT samples. Preliminary results on samples with $x = 0.46$ and 0.47, which are monoclinic at room temperature, have already been obtained. In these cases, the changes of the powder profiles induced by poling are so drastic that further work is needed in order to achieve a proper interpretation.

We thank L. Bellaiche, A.M. Glazer, J.A. Gonzalo, and K. Uchino for their stimulating discussions, B. Jones and E. Alberta for assisting in the sample preparation, and A.L. Langhorn for his invaluable technical support. Financial support by the U.S. Department of Energy under Contract No. DE-AC02-98CH10886, and by ONR under Project No. MURI (N00014-96-1-1173) is also acknowledged.

*Corresponding author.

Email address: noheda@bnl.gov

- [1] B. Jaffe, W.R. Cook, and H. Jaffe, *Piezoelectric Ceramics* (Academic Press, London, 1971).
- [2] X-h Du, U. Belegundu, and K. Uchino, *Jpn. J. Appl. Phys.* **36**, 5580 (1997).
- [3] X-h Du, J. Zheng, U. Belegundu, and K. Uchino, *Appl. Phys. Lett.* **72**, 2421 (1998).
- [4] M.J. Haun, E. Furman, S-J. Jang, and L.E. Cross, *Ferroelectrics* **72**, 13 (1989).
- [5] J. Kuwata, K. Uchino, and S. Nomura, *Jpn. J. Appl. Phys.* **21**, 1298 (1982).
- [6] S-E. Park and T.R. Shrout, *J. Appl. Phys.* **82**, 1804 (1997).
- [7] M.K. Durbin, E.W. Jacobs, J.C. Hicks, and S-E. Parks, *Appl. Phys. Lett.* **74**, 2848 (1999).
- [8] K.M. Rabe and E. Cockayne, in *Proceedings of the First-Principles Calculations for Ferroelectrics: Fifth Williamsburg Workshop*, edited by R.E. Cohen (AIP, Woodbury, 1998), p. 61.
- [9] G. Saghi-Szabo, R.E. Cohen, and H. Krakauer, *Phys. Rev. Lett.* **80**, 4321 (1998).
- [10] G. Saghi-Szabo, R.E. Cohen, and H. Krakauer, *Phys. Rev. B* **59**, 12771 (1999).
- [11] L. Bellaiche and D. Vanderbilt, *Phys. Rev. Lett.* **83**, 1347 (1999).
- [12] B. Noheda, D.E. Cox, G. Shirane, J.A. Gonzalo, L.E. Cross, and S-E. Park, *Appl. Phys. Lett.* **74**, 2059 (1999).
- [13] B. Noheda, J.A. Gonzalo, L.E. Cross, R. Guo, S-E. Park, D.E. Cox, and G. Shirane, *Phys. Rev. B* **61**, 8687 (2000).
- [14] D.L. Corker, A.M. Glazer, R.W. Whatmore, A. Stallard, and F. Fauth, *J. Phys. Condens. Matter* **10**, 6251 (1998).
- [15] S-E. Park, T.R. Shrout, P. Bridenbaugh, J. Rottenberg, and G. Loiacono, *Ferroelectrics* **207**, 519 (1998).
- [16] L. Bellaiche, A. Garcia, and D. Vanderbilt, *Phys. Rev. Lett.* (to be published).